Mechanical Integrators Derived from a Discrete Variational Principle

Jeffrey M. Wendlandt [1,2]

Mechanical Engineering, University of California at Berkeley, Berkeley, CA 94720, USA

Jerrold E. Marsden [3]

Control and Dynamical Systems, Caltech, 116-81 Pasadena, CA 91125, USA

Abstract

Many numerical integrators for mechanical system simulation are created by using discrete algorithms to approximate the continuous equations of motion. In this paper, we present a procedure to construct time-stepping algorithms that approximate the flow of continuous ODE's for mechanical systems by discretizing Hamilton's principle rather than the equations of motion. The discrete equations share similarities to the continuous equations by preserving invariants, including the symplectic form and the momentum map. We first present a formulation of discrete mechanics along with a discrete variational principle. We then show that the resulting equations of motion preserve the symplectic form and that this formulation of mechanics leads to conservation laws from a discrete version of Noether's theorem. We then use the discrete mechanics formulation to develop a procedure for constructing mechanical integrators for continuous Lagrangian systems. We apply the construction procedure to the rigid body and the double spherical pendulum to demonstrate numerical properties of the integrators.

PACS: 46.10, 02.60

Keywords: Discrete Mechanics, Symplectic Integration, Symplectic-Momentum Integration, Rigid Body Integration

[1] Ph.D. candidate; Research partially supported by DOE contract DE-FG03095ER-25251; wents@eecs.berkeley.edu; http://robotics.eecs.berkeley.edu/~wents/

[2] Corresponding author. Office (510) 643-5796 Fax (510) 642-1341. Address: UC Berkeley, EECS Dept., 211-171 Cory Hall No. 1772, Berkeley, CA 94720 USA

[3] Research partially supported by DOE contract DE-FG03095ER-25251 and the California Institute of Technology; marsden@cds.caltech.edu; http://cds.caltech.edu/~marsden/

1 Introduction

Goals. The goal of this paper is to present a systematic construction of mechanical integrators for simulating finite dimensional mechanical systems with symmetry based on a discretization of Hamilton's principle. We strive for a method that is theoretically attractive and numerically competitive. Of course, we do not claim that the methods will be superior in very specific problems for which custom methods may be available (as, for example, in symplectic integrators for the solar system—see, for example, [52]).

Mechanical Integrators. These are numerical integration methods that preserve some of the invariants of the mechanical system, such as, energy, momentum, or the symplectic form. It is well known that if the energy and momentum map include all the integrals from a certain class (depending on the smoothness available), then one cannot create integrators that are symplectic, energy preserving, *and* momentum preserving unless they coincidentally integrate the equations exactly up to a time parametrization (see [10] for the exact statement). Thus, mechanical integrators divide into two overall classes, *symplectic-momentum* and *energy-momentum* integrators. It is the hope that by exploiting the structure of mechanical systems, one can create mechanical integrators that are not only theoretically attractive, but are more computationally efficient and have better long term simulation properties than conventional integration schemes. The overall situation for mechanical integrators is of course a complex one, and it is still evolving. We refer to [28] for a recent collection of papers in the area and for additional references and to [26] for some additional background.

The Main Technique of This Paper. This paper presents a method to construct symplectic-momentum integrators for Lagrangian systems defined on a linear space with holonomic constraints. The constraint manifold, Q, is regarded as embedded in the linear space, V. A discrete version of the Lagrangian is then formed and a discrete variational principle is applied to the discrete Lagrangian system. The resulting discrete equations define an implicit (explicit in some cases) numerical integration algorithm on $Q \times Q$ that approximates the flow of the continuous Euler-Lagrange equations on TQ. The algorithm equations are called the *discrete Euler-Lagrange (DEL)* equations. We treat holonomic constraints through constraint functions on the linear space. The constraints are satisfied at each time step through the use of Lagrange multipliers.

The DEL equations share similarities to the continuous Euler-Lagrange equations. The DEL equations preserve a symplectic form defined in the paper

and preserve a discrete momentum derived through a discrete Noether's theorem. The discrete momentum corresponding to invariance of the continuous Lagrangian system to a linear group action is conserved, and the value of the discrete momentum approaches the value of the continuous momentum as the step size decreases. In general, the method does not preserve energy for conservative Lagrangian systems, but the numerical examples suggest that the energy varies about a constant value. The energy variations decrease and the constant value approaches the continuous energy as the step size decreases.

Accuracy The construction method produces 2-step methods that have a second order local truncation error. The position error in the numerical examples show second order convergence. One may be able to use the methods in [54] to increase the order of accuracy.

The Role of Dissipation. Dissipation is of course very important for practical simulations of mechanical systems. However, our philosophy, which is consistent with that of many other authors (*e.g.*, [2], [9]) is that of understanding well the ideal model first, and then one can use a time-splitting (product formula) method to interleave it with ones favorite dissipative method.

Some of the Literature. This paper uses the discrete variational principle presented in [48] and again in [49] and [32]. It is shown in [48] that the DEL equations preserve a symplectic form. The same discrete mechanics procedure is derived in [3] using an algebraic approach, and they also show that there is a discrete Noether's theorem for infinitesimal symmetry.

Various authors have proposed versions of discrete mechanics. Some study discrete mechanics without the motivation of constructing integration schemes while this is a definite motivation for other authors. In [25], the author presents a version of discrete mechanics based on the concept of a difference space. The author later shows how to derive the discrete equations from a discrete version of Hamilton's variational principle, the same discretization later used in [48]. The author in [25] also presents a version of Noether's theorem. A different approach to discrete mechanics for point mass systems not derived from a variational principle is shown in [16], [17], and [18]. These algorithms preserve energy and momentum. The author in [24] discusses methods to approximate the action integral and to use Hamilton's principle to create numerical integrators. The authors in [23] use Hamilton's principle and restricted function spaces to create integration algorithms. We prefer the approach in [48] and adopt it in this paper.

Some authors discretize the principle of least action instead of Hamilton's principle. Algorithms that conserve the Hamiltonian are derived in [14] based on difference quotients. Differentiation is not used and the action is extremized using variational difference quotients. This development presents multistep methods with variable time steps. The least action principle is discretized in a different way in [43]. The resulting equations explicitly enforce energy, and it is stated that the equations preserve quadratic invariants.

Various energy-momentum integrators have been developed by Simo and his co-workers. See, for example, [44]. Recently, energy-momentum integrators have been derived based on discrete directional derivatives and discrete versions of Hamiltonian mechanics in [12]. More references on energy-momentum methods are in the reference section of [12] and in [13]. Symplectic, momentum and energy conserving schemes for the rigid body are presented in [22].

There is a vast amount of literature on symplectic schemes for Hamiltonian systems. The overview of symplectic integrators in [40] provides background and references. See also [8] for a survey of the early work and [30] for a presentation of open problems in symplectic integration. References related to the work in this paper are [35], [36], [31], and [15]. In [35], an integration method is presented for Hamiltonian systems that enforces position and velocity constraints in such a way to make the overall method symplectic. It is shown in [36] and in [31] that the algorithm also conserves momentum corresponding to a linear symmetry group when the constraint manifold is embedded in a linear space. For another treatment of algorithms formed by embedding the constraint manifold in a linear space, see [5]. See [20] for a treatment of symplectic integration on Riemannian manifolds. The algorithm presented in this paper also embeds the constraint manifold in a linear space but only enforces position constraints.

Contributions. This paper clearly presents and develops existing results on discrete mechanics shown in [25] and in [48]. These results are then extended to create a general method to construct symplectic-momentum integrators for Lagrangian systems with holonomic constraints. An equivalent algorithm is presented in terms of generalized coordinates where the constraint equations are eliminated. This paper uses the general technique to create a symplectic-momentum integrator for the rigid body in terms of unit quaternions.

Outline of the Paper. The paper firsts presents and develops discrete mechanics in a consistent notation by presenting the discrete variational principle (DVP) and by deriving the properties of the discrete Euler-Lagrange (DEL) equations. The discrete mechanics theory is then used to develop a construction procedure for mechanical integrators. A construction procedure is pre-

sented for constrained and generalized coordinates followed by a discussion of the structure of the Jacobian relevant to solving the DEL equations. It is then shown that the DEL equations have a second order local truncation error, and that the DEL equations have a solution for a small enough time step as long as the continuous Euler-Lagrange equations are solvable. The definition for the discrete momentum is then presented. The method is applied to the rigid body (RB) to produce evolution equations in terms of unit quaternions and is applied to the double spherical pendulum (DSP). For both examples, the momentum, energy, accuracy, and efficiency is examined. We also compare the DSP integrator to an energy-momentum integrator. The paper concludes with a discussion of future work.

2 Discrete Variational Principle

A *discrete variational principle (DVP)* is presented in this section that leads to evolution equations that are analogous to the Euler-Lagrange equations. We call the evolution equations *discrete Euler-Lagrange (DEL)* equations. The results in this and the next section have appeared in [48], [49], [32] and in [3] but are rederived here in a consistent notation for completeness and clarity.

Given a configuration space, Q, a *discrete Lagrangian* is a map $\mathbb{L} : Q \times Q \to \mathbb{R}$. We later show in Equation (4.1) how to define a discrete Lagrangian given a continuous-time Lagrangian. We now give a procedure that defines the evolution map for the system. For a fixed, positive integer N, the *action sum* is the map $\mathbb{S} : Q^{N+1} \to \mathbb{R}$ defined by

$$\mathbb{S} = \sum_{k=0}^{N-1} \mathbb{L}\left(q_{k+1}, q_k\right), \tag{2.1}$$

where $q_k \in Q$ and $k \in \mathbb{Z}$ is the discrete time. The action sum is a discrete analog of the action integral. The *discrete variational principle* states that the evolution equations extremize the action sum given fixed end points, q_0 and q_N. Extremizing $\mathbb{S}$ over $q_1, \cdots, q_{N-1}$ leads to the DEL equations:

$$D_2\mathbb{L}\left(q_{k+1}, q_k\right) + D_1\mathbb{L}\left(q_k, q_{k-1}\right) = 0 \quad \text{for all } k \in \{1, \cdots, N-1\} \tag{2.2}$$

or

$$D_2\mathbb{L} \circ \Phi + D_1\mathbb{L} = 0, \tag{2.3}$$

where $\Phi : Q \times Q \to Q \times Q$ is defined implicitly by $\Phi\left(q_k, q_{k-1}\right) = \left(q_{k+1}, q_k\right)$.

If $D_2\mathbb{L}$ is invertible, then Equation (2.3) defines the discrete map, Φ, which flows the system forward in discrete time.

3 Invariance Properties

The symplectic structure of $Q \times Q$ is defined in this section and an equation for the symplectic form on $Q \times Q$ is given. It is then shown that Φ preserves the symplectic form. We then derive a discrete Noether's theorem by showing that invariance of the discrete Lagrangian leads to a conserved quantity, a momentum map, for the flow of Φ.

3.1 Symplectic Structure

We first define a fiber derivative by

$$\begin{aligned} \mathbb{FL} : Q \times Q &\to T^*Q \\ (q_1, q_0) &\mapsto (q_0, D_2\mathbb{L}(q_1, q_0)) \end{aligned} \tag{3.1}$$

and define the 2-form on $Q \times Q$ by pulling back the canonical 2-form on T^*Q:

$$\begin{aligned} \omega &= \mathbb{FL}^*(\Omega_{\mathrm{CAN}}) \\ &= \mathbb{FL}^*(-d\Theta_{\mathrm{CAN}}) \\ &= -d(\mathbb{FL}^*(\Theta_{\mathrm{CAN}})). \end{aligned} \tag{3.2}$$

The fiber derivative is analogous to the Legendre transform in continuous-time Lagrangian mechanics. Choose coordinates, q^i, on Q and choose the canonical coordinates, (q^i, p_i), on T^*Q. In these coordinates, $\Omega_{\mathrm{CAN}} = dq^i \wedge dp_i$ and $\Theta_{\mathrm{CAN}} = p_i dq^i$. The DEL equations are

$$\frac{\partial \mathbb{L}}{\partial q_k^i} \circ \Phi(q_{k+1}, q_k) + \frac{\partial \mathbb{L}}{\partial q_{k+1}^i}(q_{k+1}, q_k) = 0 \tag{3.3}$$

or

$$\frac{\partial \mathbb{L}}{\partial q_{k+1}^i}(q_{k+2}, q_{k+1}) + \frac{\partial \mathbb{L}}{\partial q_{k+1}^i}(q_{k+1}, q_k) = 0. \tag{3.4}$$

Continuing the calculations in Equation (3.2) gives

$$\omega = -d\left(\frac{\partial \mathbb{L}}{\partial q_k^i}\left(q_{k+1}, q_k\right)\right) dq_k^i \tag{3.5}$$

$$= -\frac{\partial^2 \mathbb{L}}{\partial q_k^i \partial q_{k+1}^j}\left(q_{k+1}, q_k\right) dq_{k+1}^j \wedge dq_k^i - \frac{\partial^2 \mathbb{L}}{\partial q_k^i \partial q_k^j}\left(q_{k+1}, q_k\right) dq_k^j \wedge dq_k^i \tag{3.6}$$

$$= \frac{\partial^2 \mathbb{L}}{\partial q_k^i \partial q_{k+1}^j}\left(q_{k+1}, q_k\right) dq_k^i \wedge dq_{k+1}^j, \tag{3.7}$$

since the second term in Equation (3.6) vanishes.

3.2 Preservation of the Symplectic Form

We now show that Φ preserves the symplectic form, *i.e.* $\Phi^*\omega = \omega$ where Φ^* is the pullback of Φ. For clarity, let $\Phi(y, x) = (u, v)$ and write $\omega = d(p(y, x)dx) = D_{12}\mathbb{L}(y, x)dx \wedge dy$. In this notation, $y = v = q_{k+1}$, $x = q_k$, and $u = q_{k+2}$. We now show that $\Phi^*\omega = \omega$:

$$\Phi^*\omega = \Phi^*\left(-d\left(\frac{\partial \mathbb{L}}{\partial v^i}\left(u, v\right) dv^i\right)\right) \tag{3.8}$$

$$= -d\left(\Phi^*\left(\frac{\partial \mathbb{L}}{\partial v^i}\left(u, v\right) dv^i\right)\right) \tag{3.9}$$

$$= -d\left(\frac{\partial \mathbb{L}}{\partial v^i} \circ \Phi\left(y, x\right) d\left(v^i\left(y, x\right)\right)\right) \tag{3.10}$$

$$= -d\left(-\frac{\partial \mathbb{L}}{\partial y^i}\left(y, x\right) dy^i\right) \tag{3.11}$$

$$= \frac{\partial^2 \mathbb{L}}{\partial x^j \partial y^i} dx^j \wedge dy^i \tag{3.12}$$

$$= \omega \tag{3.13}$$

We have used Equation (3.4) and the fact that $d(v(y, x)) = dy$ in deriving Equation (3.11) from Equation (3.10).

3.3 Discrete Noether's Theorem

We now derive a discrete version of Noether's theorem. For continuous-time systems, Noether's theorem states that a symmetry of the Lagrangian leads to a conserved quantity. A straight forward proof of Noether's theorem is in [42](page 102-103). Let the discrete Lagrangian be invariant under the diagonal action of a Lie group G on Q, and let $\xi \in \mathfrak{g}$ where $\mathfrak{g}$ is the Lie algebra of G. Invariance of $\mathbb{L}$ implies that

$$\mathbb{L}(\exp(s\xi)q_{k+1}, \exp(s\xi)q_k) = \mathbb{L}(q_{k+1}, q_k). \tag{3.14}$$

Differentiating Equation (3.14) and setting $s = 0$ implies that

$$D_1\mathbb{L}(q_{k+1}, q_k) \cdot \xi_Q(q_{k+1}) + D_2\mathbb{L}(q_{k+1}, q_k) \cdot \xi_Q(q_k) = 0, \tag{3.15}$$

where ξ_Q is the infinitesimal generator. Consider the action sum, Equation (2.1), where $0 < i < N$ and vary q_{k+1} over $s \in \mathbb{R}$ by $q_{k+1}(s) = \exp(s\xi)\, q_{k+1}$. Since $q_{k+1}(0)$ extremizes $\mathbb{S}$, we have

$$\left.\frac{d\mathbb{S}}{ds}\right|_{s=0} = 0. \tag{3.16}$$

Equation (3.16) implies that

$$D_1\mathbb{L}(q_{k+1}, q_k) \cdot \xi_Q(q_{k+1}) + D_2\mathbb{L}(q_{k+2}, q_{k+1}) \cdot \xi_Q(q_{k+1}) = 0. \tag{3.17}$$

Subtracting Equation (3.15) from Equation (3.17) reveals that

$$D_2\mathbb{L}(q_{k+2}, q_{k+1}) \cdot \xi_Q(q_{k+1}) - D_2\mathbb{L}(q_{k+1}, q_k) \cdot \xi_Q(q_k) = 0. \tag{3.18}$$

If we define the momentum map, $\mathbb{J} : Q \times Q \to \mathfrak{g}^*$, by

$$\langle \mathbb{J}(q_{k+1}, q_k), \xi \rangle \stackrel{\triangle}{=} \langle D_2\mathbb{L}(q_{k+1}, q_k), \xi_Q(q_k) \rangle, \tag{3.19}$$

then Equation (3.18) shows that the momentum map is preserved by $\Phi : Q \times Q \to Q \times Q$.

We note that this $\mathbb{J}$ is equivariant with respect to the action of G on $Q \times Q$ and the coadjoint action of G on $\mathfrak{g}^*$. This is proved as in the case of usual Lagrangians (see [27]). We also note that one can develop a theory of Lagrangian reduction in the discrete case, as with the continuous case (see [29]).

4 Construction of Mechanical Integrators

We show in this section how to construct mechanical integrators for continuous-time Lagrangian systems from the discrete variational principle. We first show how to construct integrators for Lagrangian systems with holonomic constraints by enforcing the constraints through Lagrange multipliers. We call this method the constrained coordinate formulation. We then present a second construction procedure by choosing a set of generalized coordinates. The

next section proves that the two methods are equivalent. We then show that the Jacobian used to solve the nonlinear equations for the constrained coordinate formulation has a special structure that can be exploited to increase simulation efficiency. Results are then presented on local truncation error and solvability. We finally relate the discrete-time momentum map and symplectic form to the continuous-time counterparts.

4.1 Constrained Coordinate Formulation

We assume that we have a mechanical system with a constraint manifold, $Q \subset V$, where V is a real, finite dimensional vector space, and that we have an *unconstrained Lagrangian*, $L : TV \to \mathbb{R}$ which, by restriction of L to TQ, defines a *constrained Lagrangian*, $L^c : TQ \to \mathbb{R}$. We also assume that we have a vector valued constraint function, $g : V \to \mathbb{R}^k$, such that $g^{-1}(0) = Q \subset V$ with 0 a regular value of g. The dimension of V is denoted n, and therefore, the dimension of Q is $m = n - k$. Also, let Λ be a real, finite dimensional vector space of Lagrange multipliers of dimension k. We first define the *discrete, unconstrained Lagrangian*, $\mathbb{L} : V \times V \to \mathbb{R}$, to be

$$\mathbb{L}(y, x) = L\left(\frac{y+x}{2}, \frac{y-x}{h}\right), \tag{4.1}$$

where $h \in \mathbb{R}_+$ is the time step. The *unconstrained action sum* is defined by

$$\mathbb{S} = \sum_{k=0}^{N-1} \mathbb{L}\left(v_{k+1}, v_k\right). \tag{4.2}$$

We then extremize $\mathbb{S} : V^{N+1} \to \mathbb{R}$ subject to the constraint that $v_k \in Q \subset V$ for $k \in \{1, \cdots, N-1\}$,

$$\begin{aligned} &\min_{v_k \in V, \lambda_k \in \Lambda} \left(\mathbb{S} + \sum_{k=1}^{N-1} \lambda_k^T g\left(v_k\right)\right) \\ &\text{subject to } g(v_k) = 0 \quad \text{for all } k \in \{1, \cdots, N-1\}, \end{aligned} \tag{4.3}$$

to derive that

$$\begin{aligned} D_2\mathbb{L}\left(v_{k+1}, v_k\right) + D_1\mathbb{L}\left(v_k, v_{k-1}\right) + \lambda_k^T Dg\left(v_k\right) = 0 \quad &\text{(no sum over } k\text{)} \\ g\left(v_k\right) = 0 \quad &\text{for all } k \in \{1, \cdots, N-1\}. \end{aligned} \tag{4.4}$$

Given v_k and v_{k-1} in $Q \subset V$, *i.e.*, $g\left(v_k\right) = 0$ and $g\left(v_{k-1}\right) = 0$, we need to solve the following equations

$$\begin{aligned} D_2\mathbb{L}\left(v_{k+1}, v_k\right) + D_1\mathbb{L}\left(v_k, v_{k-1}\right) + \lambda_k^T Dg\left(v_k\right) &= 0 \\ g\left(v_{k+1}\right) &= 0 \end{aligned} \tag{4.5}$$

for v_{k+1} and λ_k.

In terms of the original, unconstrained Lagrangian, Equation (4.5) reads as follows:

$$\begin{aligned} \frac{1}{h}\left[\frac{\partial L}{\partial \dot{v}}\left(\frac{v_k+v_{k-1}}{2},\frac{v_k-v_{k-1}}{h}\right)-\frac{\partial L}{\partial \dot{v}}\left(\frac{v_{k+1}+v_k}{2},\frac{v_{k+1}-v_k}{h}\right)\right]+ \\ \frac{1}{2}\left[\frac{\partial L}{\partial v}\left(\frac{v_k+v_{k-1}}{2},\frac{v_k-v_{k-1}}{h}\right)+\frac{\partial L}{\partial v}\left(\frac{v_{k+1}+v_k}{2},\frac{v_{k+1}-v_k}{h}\right)\right] \\ +D^T g\left(v_k\right)\lambda_k=0 \\ g\left(v_{k+1}\right)=0. \end{aligned} \tag{4.6}$$

For example, if the continuous Lagrangian system is of the form

$$\begin{aligned} L(q,\dot{q}) &= \frac{1}{2}\dot{q}^T M\dot{q}-V(q) \\ g(q) &= 0, \end{aligned} \tag{4.7}$$

where M is a constant mass matrix, and V is the potential energy, then the DEL equations are

$$\begin{aligned} M\left(\frac{v_{k+1}-2v_k+v_{k-1}}{h^2}\right)+\frac{1}{2}\left(\frac{\partial V}{\partial q}\left(\frac{v_{k+1}+v_k}{2}\right)+\frac{\partial V}{\partial q}\left(\frac{v_k+v_{k-1}}{2}\right)\right) \\ -D^T g\left(v_k\right)\lambda_k=0 \\ g\left(v_{k+1}\right)=0. \end{aligned} \tag{4.8}$$

We also note that one can obtain the algorithm in Equation (4.6) with no constraints by using $-\mathbb{L}$ as a generating function of type 1.

We now compare the constraint algorithm in Equation (4.8) to algorithms used in molecular dynamics simulation and give a brief background of these algorithms. The *Verlet* algorithm [47] is important in molecular dynamics simulation [21]. An extension of the *Verlet* algorithm to handle holonomic constraints is SHAKE [39]. SHAKE was extended to handle velocity constraints with RATTLE [1]. For a presentation of the symplectic nature of the *Verlet*, SHAKE, and RATTLE algorithms, see [21]. The construction method developed here when applied to a Lagrangian of the form in Equation (4.7) produces an integration method similar to the SHAKE algorithm written in terms of position coordinates. However, the potential force terms differ as can be seen in Equation (4.8). If one applies the construction procedure with the discrete Lagrangian definition in Equation (4.16), then one can reproduce the SHAKE algorithm. One recovers the *Verlet* algorithm if the Lagrangian system has no constraints. This result also appears in [11], and the discrete variational principle they apply is similar to the principle in [48]. However, they don't extend the result to constraints or more general Lagrangians and do not use

the discrete Lagrangian definition in this paper. The emphasis in [11] is also on calculating a path given end point conditions. Our procedure can handle more general Lagrangians, such as the Lagrangian for the rigid body in terms of quaternions.

4.2 Generalized Coordinate Formulation

For the generalized coordinate formulation, we form the discrete Lagrangian and the action sum restricted to $Q \subset V$, and then perform the extremization directly on Q by using a coordinate chart. The *constrained, discrete Lagrangian* is given by

$$\mathbb{L}^c : Q \times Q \to \mathbb{R}, \tag{4.9}$$

where $\mathbb{L}^c = \mathbb{L}|_{Q\times Q}$. Given a local coordinate chart, $\psi : U \subset \mathbb{R}^m \to Q \subset V$, where U is an open set in $\mathbb{R}^m$, the *constrained, discrete Lagrangian* is

$$\begin{aligned}\mathbb{L}^c\left(q_{k+1}, q_k\right) &= \mathbb{L}\left(\psi\left(q_{k+1}\right), \psi\left(q_k\right)\right) \\ &= L\left(\frac{\psi\left(q_{k+1}\right) + \psi\left(q_k\right)}{2}, \frac{\psi\left(q_{k+1}\right) - \psi\left(q_k\right)}{h}\right),\end{aligned}$$

where each q_k is in U. With an abuse of notation, we represent the restricted function and its representation in a coordinate chart by the same symbol. The *constrained action sum* is

$$\mathbb{S}^c = \sum_{k=0}^{N-1} \mathbb{L}^c\left(q_{k+1}, q_k\right). \tag{4.10}$$

Extremizing $\mathbb{S}^c : Q^{N+1} \to \mathbb{R}$ gives the discrete Euler-Lagrange (DEL) equations in terms of generalized coordinates,

$$D_2\mathbb{L}^c\left(q_{k+1}, q_k\right) + D_1\mathbb{L}^c\left(q_k, q_{k-1}\right) = 0. \tag{4.11}$$

In terms of the original, unconstrained Lagrangian, Equation (4.11) equals

$$\begin{aligned}D^T\psi\left(q_k\right)\Bigg\{\frac{1}{h}\left[\frac{\partial L}{\partial \dot{v}}\left(a_k, d_k\right) - \frac{\partial L}{\partial \dot{v}}\left(a_{k+1}, d_{k+1}\right)\right] \\ + \frac{1}{2}\left[\frac{\partial L}{\partial v}\left(a_k, d_k\right) + \frac{\partial L}{\partial v}\left(a_{k+1}, d_{k+1}\right)\right]\Bigg\} = 0,\end{aligned} \tag{4.12}$$

where

$$a_k = \frac{\psi\left(q_k\right) + \psi\left(q_{k-1}\right)}{2} \qquad \text{and} \qquad d_k = \frac{\psi\left(q_k\right) - \psi\left(q_{k-1}\right)}{h}. \tag{4.13}$$

We solve Equations (4.12) for q_{k+1} given q_k and q_{k-1} to advance the flow one time step.

4.3 Equivalence of the Formulations

This section proves the equivalence between the constrained and generalized coordinate formulations.

Theorem 1 *Let g be the constraint function and ψ be the coordinate chart defined above. Let q_k and q_{k-1} be the two initial points in the coordinate chart and let $v_k = \psi(q_k)$ and $v_{k-1} = \psi(q_{k-1})$. Let $Dg(v_k)$ and $D\psi(q_k)$ be full rank. Then the generalized formulation, Equation (4.12), has a solution for q_{k+1} if and only if the constrained formulation, Equation (4.6), has a solution for v_{k+1} and λ_k. Furthermore, $v_{k+1} = \psi(q_{k+1})$.*

Proof. ($\Leftarrow$) We assume that we have a solution for v_{k+1} for the constrained formulation. Let $q_{k+1} = \psi^{-1}(v_{k+1})$ and we will show that q_{k+1} solves Equation (4.12). Multiply the top equation in Equation (4.6) on the left by $D^T\psi(q_{k+1})$. Also, substitute $v_k = \psi(q_k)$ and $v_{k-1} = \psi(q_{k-1})$ into Equation (4.6). Notice that $g(\psi(q_k)) = 0$ which implies that $Dg(\psi(q_k))D\psi(q_k) = 0$. Using the substitutions and the fact that $D^T\psi(q_k)D^Tg(\psi(q_k)) = 0$ proves that q_{k+1} is a solution for Equation (4.12).

($\Rightarrow$) To complete the proof, we assume that q_{k+1} is a solution for Equation (4.12) and show that there exists a Lagrange multiplier, λ_k, so that $v_{k+1} = \psi(q_{k+1})$ is a solution for Equation (4.6). Substitute the expressions for v_{k+1}, v_k, and v_{k-1} into Equation (4.6). The lower equation in Equation (4.6) is solved automatically since $v_{k+1} \in Q$. Note that $T_{v_k}V = \mathcal{R}(D\psi(q_k)) \oplus \mathcal{N}(D^T\psi(q_k))$ and that $\mathcal{R}(D^Tg(v_k)) \subset \mathcal{N}(D^T\psi(q_k))$. Since $D^Tg(v_k)$ is full rank and $\dim(\mathcal{R}(D^Tg(v_k))) = \dim(\mathcal{N}(D^T\psi(q_k)))$, $\mathcal{R}(D^Tg(v_k))$ equals $\mathcal{N}(D^T\psi(q_k))$. We then split the left-hand side in Equation (4.6) into a component in $\mathcal{R}(D\psi(q_k))$ and an orthogonal component in $\mathcal{N}(D^T\psi(q_k))$. The component in $\mathcal{R}(D\psi(q_k))$ is zero by Equation (4.12) and the fact that $\mathcal{R}(D^Tg(v_k)) = \mathcal{N}(D^T\psi(q_k))$. We can then find a Lagrange multiplier, λ_k, to make the component in $\mathcal{N}(D^T\psi(q_k))$ equal to zero since $\mathcal{R}(D^Tg(v_k)) = \mathcal{N}(D^T\psi(q_k))$. Therefore, there exists a λ_k so that $v_{k+1} = \psi(q_{k+1})$ solves Equation (4.6). $\square$

In Figure 1, we illustrate the relationships between constrained and generalized coordinate formulations for discrete-time mechanics as well as continuous-time mechanics. The figure also points out where the discrete-time equations approximate the flow of the continuous-time equations. The results for continuous-time mechanics are summarized on the left side of the figure. We

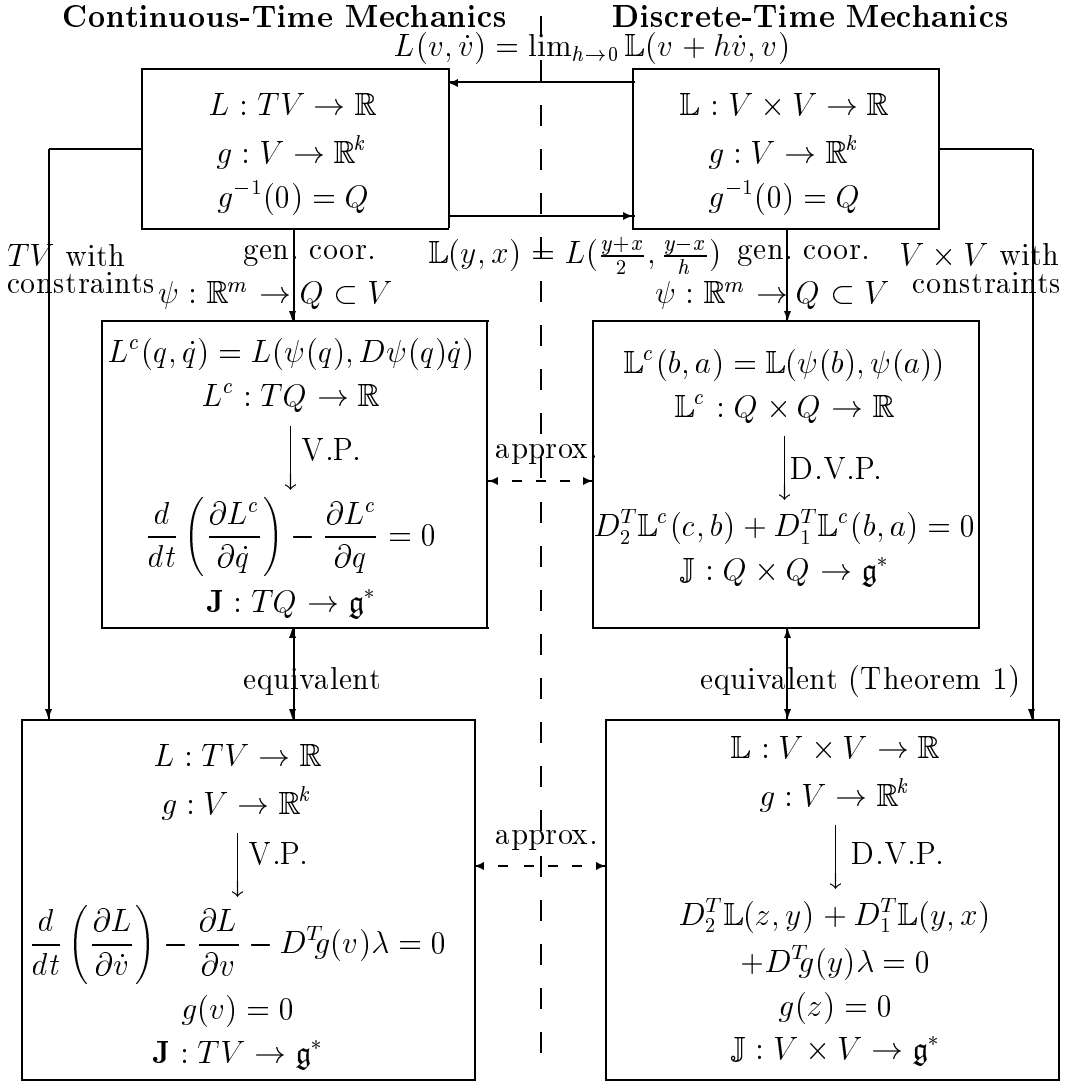

Fig. 1. Comparison of Continuous and Discrete Formulations of Mechanics

assume we are given an unconstrained Lagrangian with constraint functions as shown in the upper left corner. One can use generalized coordinates and apply Hamilton's principle to produce the Euler-Lagrange equations or one can use constrained coordinates and enforce the constraints through Lagrange multipliers. The right side of the figure summarizes the results for discrete-time mechanics. Given the continuous, unconstrained Lagrangian, one can form the discrete, unconstrained Lagrangian. One can proceed analogously to continuous-time mechanics by using generalized or constrained coordinates. We discuss in Section 4.5 how the discrete equations approximate the continuous-time equations.

4.4 Jacobian Structure

For the numerical examples presented later in this paper, we solve the DEL equations, Equation (4.5), using Newton-Raphson equation solvers. These solvers require the construction of a Jacobian formed by differentiating Equation (4.5) with respect to v_{k+1} and λ_k to get

$$J(v_{k+1}, v_k, h) = \begin{bmatrix} D_{12}\mathbb{L}(v_{k+1}, v_k) & D^T g(v_k) \\ Dg(v_{k+1}) & 0 \end{bmatrix}, \tag{4.14}$$

where

$$[D_{12}\mathbb{L}(v_{k+1}, v_k)]_{ij} = \frac{\partial^2 \mathbb{L}}{\partial v_k^i \partial v_{k+1}^j}(v_{k+1}, v_k).$$

For many applications, the nearly symmetric Jacobian, Equation (4.14), is a sparse matrix and sparse matrix techniques can be used in the Newton-Raphson steps to increase the simulation efficiency. For tree structured multibody systems, one can show that the linear equations involving the Jacobian can be solved in linear time. The authors in [5] particulate the rigid bodies in a multibody system with point masses. They then use symplectic-momentum integrators with constraints and general sparse matrix techniques to simulate multibody systems. The author in [38] uses the methods in [37] to create symplectic-momentum integrators for multibody systems.

4.5 Local Truncation Error and Solvability

Results on truncation error and solvability are presented in this section. We follow the definition of local truncation error in [19](page 56). To calculate the truncation error, we first insert an exact solution of the differential equations into the algorithm equations in Equation (4.12), and then expand the resulting equation in terms of the step size h. To calculate the expansion, it is easier to first expand Equation (4.12) about

$$v_k^i = \psi^i(q_k) \qquad \text{and} \qquad \dot{v}_k^i = \frac{\partial \psi^i}{\partial q_k^j}\dot{q}_k^j, \tag{4.15}$$

and then expand the result into powers of h. This lengthy calculation which we do not reproduce here reveals that the local truncation error of the method is second order. The first term, h^0, is zero since $q, \dot{q}$ satisfy the continuous Euler-Lagrange equations. The second term, h^1, is zero through a cancellation of terms. The h^2 term is non-zero, and the coefficient is a lengthy expression involving second, third, and fourth partial derivatives of $L : TV \to \mathbb{R}$.

If one uses the following definition for the discrete Lagrangian:

$$\mathbb{L}(y, x) = L(y, \frac{y - x}{h}), \tag{4.16}$$

then the resulting DEL equations will only be first order accurate for a general Lagrangian. There is no cancellation of terms in the h^1 term as there is with the definition in Equation (4.1). However, in some cases, the resulting DEL equations may be explicit while the DEL equations from the definition in Equation (4.1) are implicit. An example of this occurring is if the continuous Lagrangian is in the form in Equation (4.7), and there are no constraints.

The existence of a solution for the continuous-time equations is related to the solvability of the generalized coordinate discrete equations. One can show that if $D_{22}L$ is non-singular and if the Jacobian of the constraints is full rank, then for a sufficiently small time step, the generalized coordinate DEL equations are solvable for q_{k+1}. This is proved by showing that the DEL equations have a solution for $h = 0$ by taking the limit and then by using the implicit function theorem to conclude that there is a solution in a neighborhood of $h = 0$. Theorem 1 then implies that there is also a solution for the DEL equations with Lagrange multipliers.

4.6 Symplectic Form and Discrete Momentum Map

The integrators created through the construction procedure are symplectic-momentum integrators; however, this statement requires clarification which we present in this section. The integrators are symplectic in that the map produced on T^*V or T^*Q is a symplectic map. Also, if the Lie group acts linearly on V, then the continuous flow of the Euler-Lagrange equations and the discrete map produced from the DEL equations preserve the same momentum map on T^*Q.

However, if one integrates the continuous equations exactly or accurately and uses the result to initialize the discrete equations, one will notice that the *value* of the momentum map will differ from the value of the momentum map for the continuous system. The difference arises from the difference in the assignment of the momentum coordinate in T^*V through the fiber derivative. In the continuous case, the momentum is D_2L while in the discrete case, we choose to use $-hD_2\mathbb{L}$. We multiply by a $-h$ from the definitions given in Equation (3.1) because $-hD_2\mathbb{L}$ converges to D_2L as $h \to 0$.

If the Lagrangian of a continuous system is invariant to the action of a group,

and if the constraints are also invariant under the group action, *i.e.*

$$\begin{gathered} L : TV \to \mathbb{R} \\ L\left(G \cdot v, G \cdot \dot{v}\right) = L\left(v, \dot{v}\right) \\ g\left(G \cdot v\right) = g\left(v\right), \end{gathered}$$

where the action of G on $v \in V$ is represented as $G \cdot v$, then the flow of the Euler-Lagrange equations preserve the momentum map,

$$\mathbf{J} : TV \to \mathfrak{g}^*,$$

where

$$\left\langle \mathbf{J}\left(v, \dot{v}\right), \xi \right\rangle \triangleq \left\langle \frac{\partial L}{\partial \dot{v}}\left(v, \dot{v}\right), \xi_V(v) \right\rangle.$$

If the group G also acts linearly on V, then the discrete Lagrangian is also invariant to the group action through the following calculation:

$$\begin{aligned} \mathbb{L}\left(G \cdot v_{k+1}, G \cdot v_k\right) &= L\left(\frac{G \cdot v_{k+1} + G \cdot v_k}{2}, \frac{G \cdot v_{k+1} - G \cdot v_k}{h}\right) \\ &= L\left(G \cdot \left(\frac{v_{k+1} + v_k}{2}\right), G \cdot \left(\frac{v_{k+1} - v_k}{h}\right)\right) \\ &= L\left(\frac{v_{k+1} + v_k}{2}, \frac{v_{k+1} - v_k}{h}\right) \\ &= \mathbb{L}\left(v_{k+1}, v_k\right). \end{aligned}$$

From a similar derivation to the derivation in Section (3.3), one can show that the following momentum map

$$\mathbb{J} : V \times V \to \mathfrak{g}^*$$

defined by the relation

$$\left\langle \mathbb{J}(v_{k+1}, v_k), \xi \right\rangle \triangleq \left\langle D_2\mathbb{L}(v_{k+1}, v_k), \xi_V(v_k) \right\rangle$$

is conserved by the flow of the DEL equations.

We now calculate $-hD_2\mathbb{L}$ and notice

$$\begin{gathered} -hD_2\mathbb{L}\left(v_{k+1}, v_k\right) = -h\frac{\partial}{\partial v_k}\left(L\left(\frac{v_{k+1} + v_k}{2}, \frac{v_{k+1} - v_k}{h}\right)\right) \\ = \frac{\partial L}{\partial \dot{v}}\left(\frac{v_{k+1} + v_k}{2}, \frac{v_{k+1} - v_k}{h}\right) - \frac{h}{2}\frac{\partial L}{\partial v}\left(\frac{v_{k+1} + v_k}{2}, \frac{v_{k+1} - v_k}{h}\right). \end{gathered}$$

As $h \to 0$, the discrete momentum value, $-hD_2\mathbb{L}$, converges to the continuous momentum value, D_2L. Therefore, the quantities that depend on the discrete momentum value, such as the *discrete momentum map* defined to be $-h\mathbb{J}$, converge to their continuous counterparts as $h \to 0$.

5 Numerical Examples

We apply the construction procedure to produce mechanical integrators for the rigid body (RB) and the double spherical pendulum (DSP). We choose to use constrained coordinates instead of generalized coordinates to avoid coordinate singularities and coordinate patching. We use unit quaternions to create the rigid body algorithm, and use the position of the two masses for the double spherical pendulum. We compare the double spherical pendulum algorithm to an energy-momentum algorithm presented in [50] based on the work in [12].

In the simulations, we use energy as a monitor to catch any obvious problems, as in [8] and [45]. It is still unknown if this is a reliable indicator, but based on the Ge-Marsden result mentioned before, it may well be. Another indication is the analysis with energy oscillation and nearby Hamiltonian systems in [40](page 277–278), [41](page 139–140), and [6]. We must note, however, that energy conservation alone does not imply good performance as is shown in [34]. In our examples, we observe energy oscillations around a constant value, which we take as a good indication.

When comparing energy-momentum and symplectic-momentum methods, it should be kept in mind that energy-momentum methods should be monitored using how well they conserve the symplectic form. This is of course not so straightforward as monitoring using the energy, since the symplectic condition involves computing the derivative of the flow map (*e.g.*, using a cloud of initial conditions). We do not directly address these questions, but it is important to keep them in mind.

5.1 Rigid Body

The algorithm presented here updates quaternion variables based on the previous two quaternion variables. The configuration manifold is taken to be $Q = S^3 \subset V$ where $V = \mathbb{R}^4$. Quaternions were used instead of using $V = \mathbb{R}^9$ with the six orthogonal constraints of $SO(3)$ primarily to avoid a large number of Lagrange multipliers. The constraint function is $g(v) = v \cdot v - 1$ and is enforced with a Lagrange multiplier. The use of generalized coordinates to eliminate the use of Lagrange multipliers introduces the problem of coordinate switching.

Rigid body integrators that preserve certain mechanical properties have been created by several researchers. A symplectic integrator which preserves the momentum and energy is presented in [22]. An energy-momentum integrator is presented in [46]. A symplectic-momentum integrator is presented in [31]. A rigid body integrator based on a discrete variational principle and in terms of

3×3 matrices with constraints is presented in [32]. It would be interesting to compare in more detail the integrator in [32] to the quaternion-based integrator in this section.

We first attach a body frame to the rigid body and represent the frame as a matrix, $R \in SO(3)$, which maps vectors in the body frame, $\mathcal{B}$, to vectors in the spatial (inertial) frame, $\mathcal{S}$. The rotation matrix is then thought of as a mapping, $R : \mathcal{B} \to \mathcal{S}$.

We now present a background in quaternions. Consult [33] for more information on quaternions. A unit quaternion is a four parameter representation of $SO(3)$. The quaternion consists of a scalar value, q_s, and a vector with three components which we denote $q_v = (q_x, q_y, q_z)$. The following formula constructs a $SO(3)$ matrix, R, from its unit quaternion representation, q:

$$R = (2q_s^2 - 1)I + 2q_s\hat{q}_v + 2q_v q_v^T, \tag{5.1}$$

where

$$\hat{q}_v = \begin{bmatrix} 0 & -q_z & q_y \\ q_z & 0 & -q_x \\ -q_y & q_x & 0 \end{bmatrix}. \tag{5.2}$$

A useful property of the unit quaternion representation is that if A, B, and $C \in SO(3)$ are represented by unit quaternions, a, b, and c, respectively, then $C = AB$ if and only if $c = \pm a \star b$ where $\star$ represents quaternion multiplication. If $c = a \star b$, then $c_s = a_s b_s - a_v \cdot b_v$ and $c_v = a_s b_v + b_s a_v + a_v \times b_v$. Also, the conjugate of a denoted $\bar{a}$ is given by $\bar{a} = (a_s, -a_v)$. For unit quaternions, $\bar{a}$ is the inverse of a, in that $a \star \bar{a} = (1, 0, 0, 0)$. An additional fact about quaternions is that if $w = Av$ and a is a unit quaternion that represents A, then $(0, w) = a \star (0, v) \star \bar{a}$ where $(0, w)$ is a quaternion formed from the vector w.

If $R : \mathcal{B} \to \mathcal{S}$ is the rotation matrix representing the orientation of the rigid body, then the body angular velocity vector, ω_b, is given by $\hat{\omega}_b = R^T \dot{R}$. Another fact about quaternions is that if r is the unit quaternion representing R, then $\bar{r} \star \dot{r} = (0, \omega_b/2)$.

Using the above relationship for the body angular velocity, we construct the continuous Lagrangian, $L : TV \to \mathbb{R}$, to be

$$L(q, \dot{q}) = \frac{1}{2}(2\overline{q} \star \dot{q})^T \begin{bmatrix} 0 & 0 \\ 0 & \mathbb{I} \end{bmatrix} (2\overline{q} \star \dot{q}), \tag{5.3}$$

where $\mathbb{I}$ is the inertia matrix. The constraint is the unit norm constraint for quaternions, $q_s^2 + q_v \cdot q_v = 1$.

The Lagrangian in Equation (5.3) is invariant under left quaternionic multiplication, *i.e.*

$$L\left(r \star q, r \star \dot{q}\right) = L\left(q, \dot{q}\right),$$

where r is a unit quaternion. The invariance leads to conservation of angular momentum.

The discrete Lagrangian, $\mathbb{L} : TV \to \mathbb{R}$, is chosen to be

$$\mathbb{L}(y, x) = L\left(\frac{y+x}{2}, \frac{y-x}{h}\right). \tag{5.4}$$

We first simplify the body angular velocity term to get

$$2\overline{q} \star \dot{q} \mapsto \left(\overline{\frac{y+x}{2}}\right) \star \left(\frac{y-x}{h}\right) \tag{5.5}$$

$$= \frac{1}{h}(\overline{y} \star y - \overline{y} \star x + \overline{x} \star y - \overline{x} \star x). \tag{5.6}$$

Restricted to Q, $\overline{y} \star y = \overline{x} \star x = (1, 0, 0, 0)$. Simplifying restricted to Q gives

$$2\overline{q} \star \dot{q} \mapsto \frac{1}{h}(\overline{x} \star y - \overline{y} \star x). \tag{5.7}$$

Equation (5.7) is an approximation to the body angular velocity, $(0, \omega_b)$. The simplified discrete Lagrangian restricted to Q is then

$$\mathbb{L}(y, x) = \frac{1}{2h^2}(\overline{x} \star y - \overline{y} \star x)^T \begin{bmatrix} 0 & 0 \\ 0 & \mathbb{I} \end{bmatrix} (\overline{x} \star y - \overline{y} \star x), \tag{5.8}$$

and the discrete Lagrangian on all of $V \times V$ is then taken to be equal to Equation (5.8). Since we are extremizing $\mathbb{S}$ restricted to Q, the extension of $\mathbb{L}$ to $V \setminus Q$ is arbitrary.

The discrete Lagrangian in Equation (5.8) is also invariant under left quaternionic multiplication, *i.e.*

$$\mathbb{L}\left(r \star y, r \star x\right) = \mathbb{L}\left(y, x\right),$$

where r is a unit quaternion, and the invariance leads to conservation of discrete momentum which converges to the continuous momentum as the step size decreases, as we have seen.

The DEL equations for the RB and relevant Jacobian are created in Mathematica [53] and exported to C-code for simulation. The initial conditions and RB parameters are

$$q_0 = \begin{bmatrix} 1 \\ 0 \\ 0 \\ 0 \end{bmatrix} \qquad \omega_b = \begin{bmatrix} 0 \\ 3 \\ 4 \end{bmatrix} \qquad \mathbb{I} = \begin{bmatrix} 1 & 0 & 0 \\ 0 & 2 & 0 \\ 0 & 0 & 3 \end{bmatrix}. \tag{5.9}$$

We must first initialize the rigid body integrator by choosing two initial quaternion values. We do this by using an Euler step with $\dot{q} = q \star (0, \omega_b/2)$ with $h = 10^{-5}$s. We then use the DVP integrator with $h = 10^{-5}$s to set the second initial point for $h = 10^{-4}$s, 10^{-3}s, 10^{-2}s, and 10^{-1}s. The system is simulated for 30 seconds. To calculate errors in energy, momentum, and position, we first choose a standard value. We use the energy and momentum given initially after the first Euler step at $h = 10^{-5}$s as the standard energy and momentum values. We use the results of the 30s simulation with $h = 10^{-4}$s as the standard position variables. We use the following formula to calculate errors for each simulation:

$$\text{error} = \frac{1}{Nm} \sum_{i=1}^{N} \parallel v_i - v_i^s \parallel_2, \tag{5.10}$$

where m is the length of the vector v_i, v_i^s is the standard value at the ith sample, and N is the number of samples. The results of the simulations are tabulated in Table 5.1. The table lists CPU time on a SGI Indy (1 100 MHZ IP22 Processor, FPU: MIPS R4610 Floating Point, CPU:MIPS R4600 Processor), quaternion error, energy error, and momentum error.

Table 1
Simulation Results for the Rigid Body Simulation

h (s)	CPU time (s)	Quat. Error	Energy Error	Mom. Error
0.0001	97.620	0.0	6.256e-7	1.671e-7
0.001	9.905	3.960e-6	6.274e-5	1.687e-5
0.01	1.397	3.997e-4	6.274e-3	1.687e-3
0.1	0.301	3.648e-2	6.217e-1	1.665e-1

Figure 2 is a log-log plot of CPU time in seconds versus time step in seconds. The CPU time drops off nearly linearly as the time step increases. The CPU time is corrected for the time it takes to initialize each simulation with the $h = 10^{-5}$s simulation.

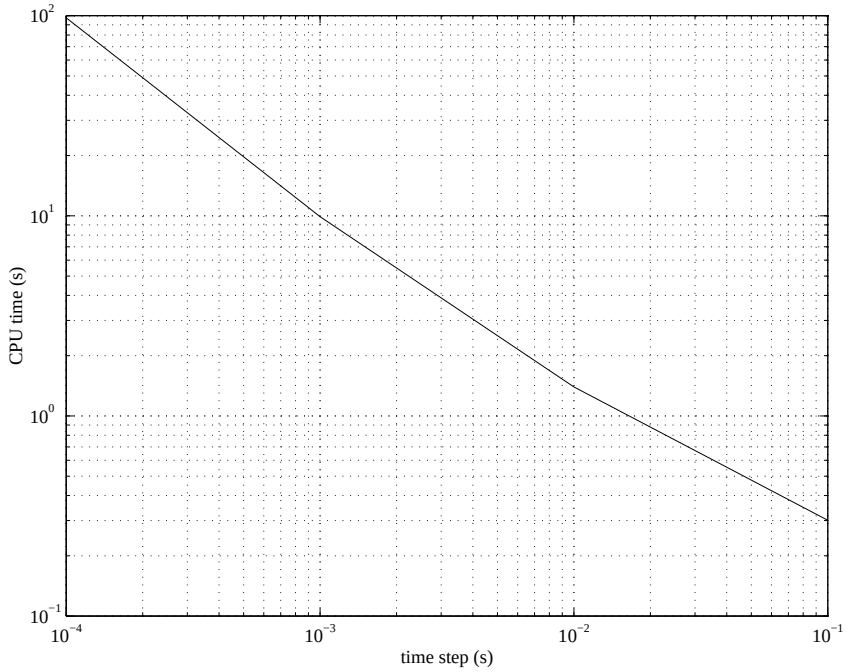

Fig. 2. CPU Time Versus Time Step for the Rigid Body Simulation

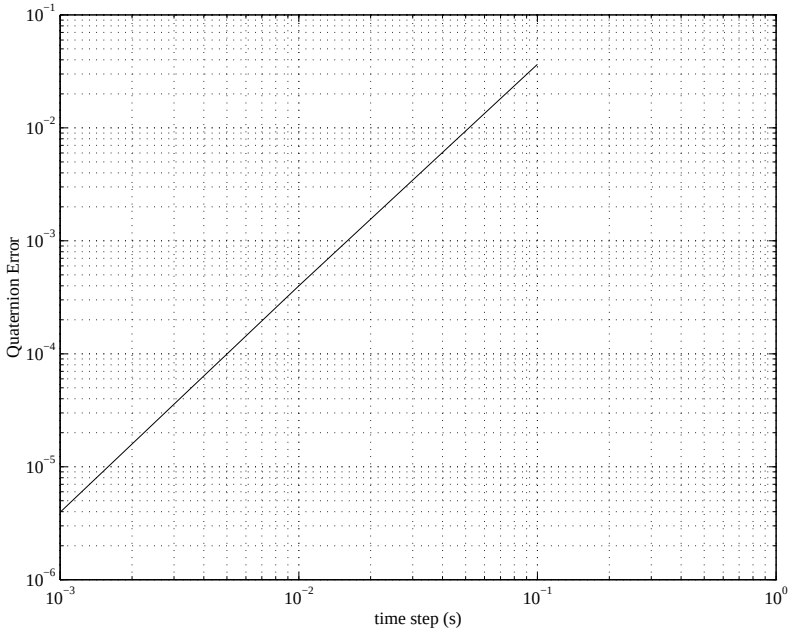

Fig. 3. Quaternion Error Versus Time Step

The quaternion error versus time step is shown in Figure 3. The plot shows a second order relationship between error and time step.

Figure 4 compares the plot of the quaternion, q_y, versus time for the simulations at $h = 10^{-4}$s and $h = 10^{-1}$s. The trajectory for the large time step

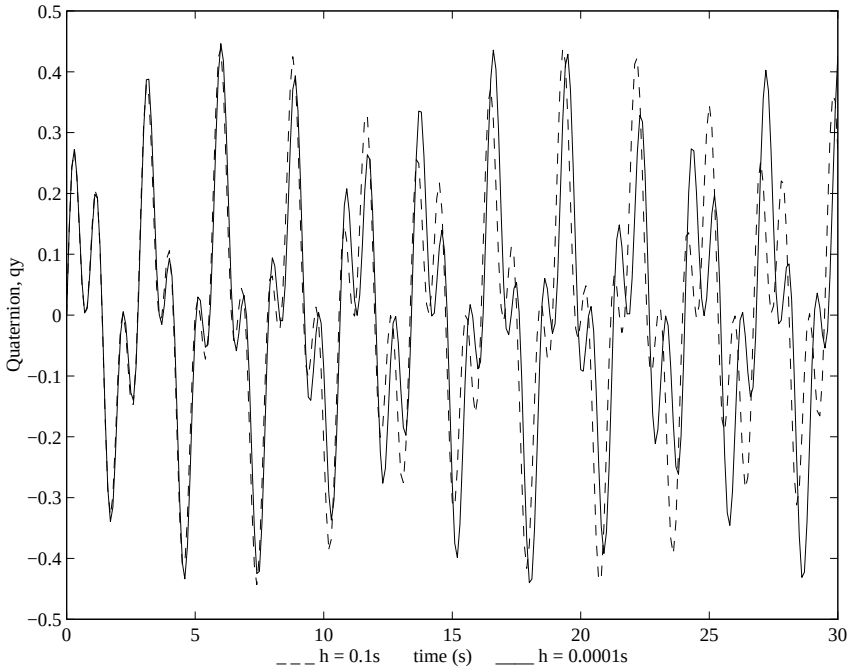

Fig. 4. Quaternion Coordinate Versus Time

exhibits the same qualitative behavior as the small time step, but the deviations increase for longer simulation times.

The energy error versus time step is shown in Figure 5. The figure reveals a second order relationship between energy error and time step. The energy for the $h = 10^{-4}$s simulation deviates between 32.99999935$\underline{9}$J and 32.99999934$\underline{9}$J. The energy for the simulation at $h = 10^{-3}$s deviates between 32.9999372$\underline{36}$J and 32.9999372$\underline{35}$J. There is no deviation in energy for the $h = 10^{-2}$s and $h = 10^{-1}$s simulations.

For each time step, the constant value of the discrete momentum map is conserved; however, as explained in Section 4.6, the value converges to the continuous momentum value as the step size decreases. The convergence of the discrete momentum is shown in Figure 6. The figure reveals a second order relationship between momentum error and time step. The angular momentum for each simulation should remain constant, but there are small deviations ($\pm 10^{-9}$) in the data for the $h = 10^{-4}$s simulation. There are no deviations in the momentum value for the other simulations.

5.2 Double Spherical Pendulum

The double spherical pendulum consists of two constrained point masses. The configuration space is $Q = S^2 \times S^2$ and the linear space is $V = \mathbb{R}^3 \times \mathbb{R}^3$. The position of the first mass is $q_1 = (x_1, y_1, z_1)$, and the position of the second

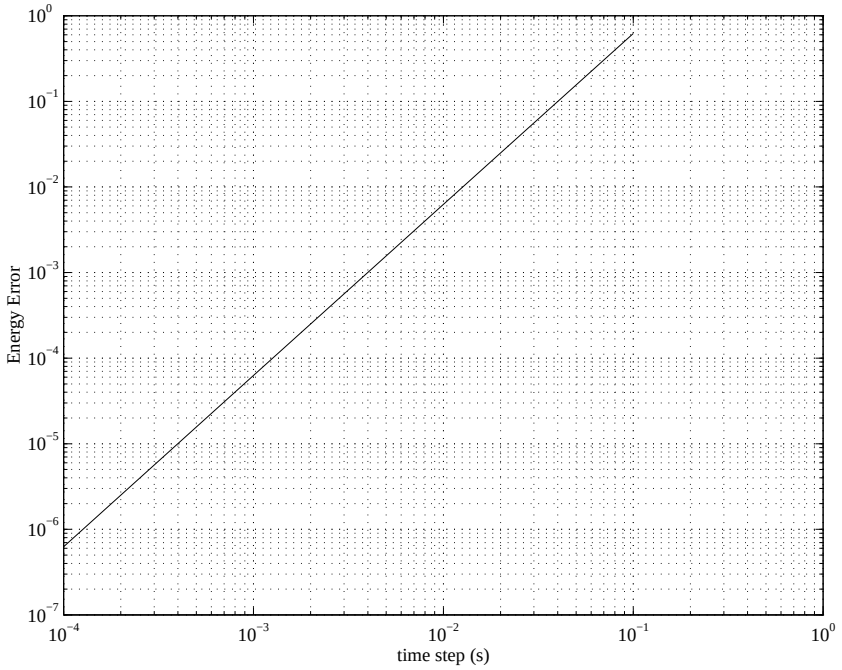

Fig. 5. Energy Error Versus Time Step for the Rigid Body Simulation

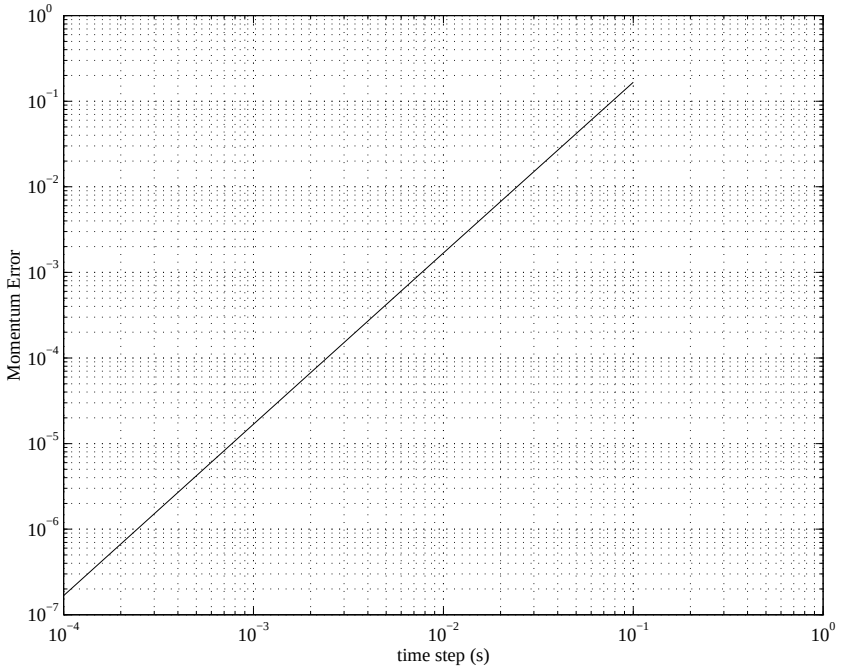

Fig. 6. Momentum Error Versus Time Step for the Rigid Body Simulation

mass is $q_2 = (x_2, y_2, z_2)$. The constraint equation, given by the pendulum length constraints, is

$$g(v) = \begin{bmatrix} q_1 \cdot q_1 - l_1^2 \\ (q_2 - q_1) \cdot (q_2 - q_1) - l_2^2 \end{bmatrix}. \tag{5.11}$$

The DSP Lagrangian system is of the form in Equation (4.7), and the DEL equations for this system are of the form in Equation (4.8). The DVP algorithm for the DSP is the SHAKE algorithm:

$$\frac{1}{h}M\left[q^{n+1}-2q^{n}+q^{n-1}\right]+h\begin{bmatrix}0\\0\\m_1\mathrm{g}\\0\\0\\m_2\mathrm{g}\end{bmatrix}-hD^{T}g\left(q^{n}\right)\lambda=0$$
$$g\left(q^{n+1}\right)=0,$$

where

$$M=\begin{bmatrix}m_1I & 0\\ 0 & m_2I\end{bmatrix},\qquad q=\begin{bmatrix}q_1\\q_2\end{bmatrix}, \tag{5.12}$$

and m_1 and m_2 are the masses.

We compare the simulation from the discrete variational principle (DVP) construction to an energy-momentum (EM) formulation based on the construction procedure in [12], and applied to the DSP in [50]. The EM algorithm for the DSP is

$$q_1^{n+1}-q_1^{n}-h\frac{1}{m_1}p_1^{n+\frac{1}{2}}=0$$
$$q_2^{n+1}-q_2^{n}-h\frac{1}{m_2}p_2^{n+\frac{1}{2}}=0$$
$$p^{n+1}-p^{n}+h\left[\begin{bmatrix}0\\0\\m_1\mathrm{g}\\0\\0\\m_2\mathrm{g}\end{bmatrix}+\lambda_1\begin{bmatrix}q_1^{n+1}+q_1^{n}\\0\end{bmatrix}+\lambda_2\begin{bmatrix}q_1^{n+1}+q_1^{n}-q_2^{n+1}-q_2^{n}\\q_2^{n+1}+q_2^{n}-q_1^{n+1}-q_1^{n}\end{bmatrix}\right]=0$$
$$\left(q_1^{n+1}\right)\cdot\left(q_1^{n+1}\right)-l_1^2=0$$
$$\left(q_2^{n+1}-q_1^{n+1}\right)\cdot\left(q_2^{n+1}-q_1^{n+1}\right)-l_2^2=0,$$

where p_i is the momentum for the ith mass, p is the six vector of momentum

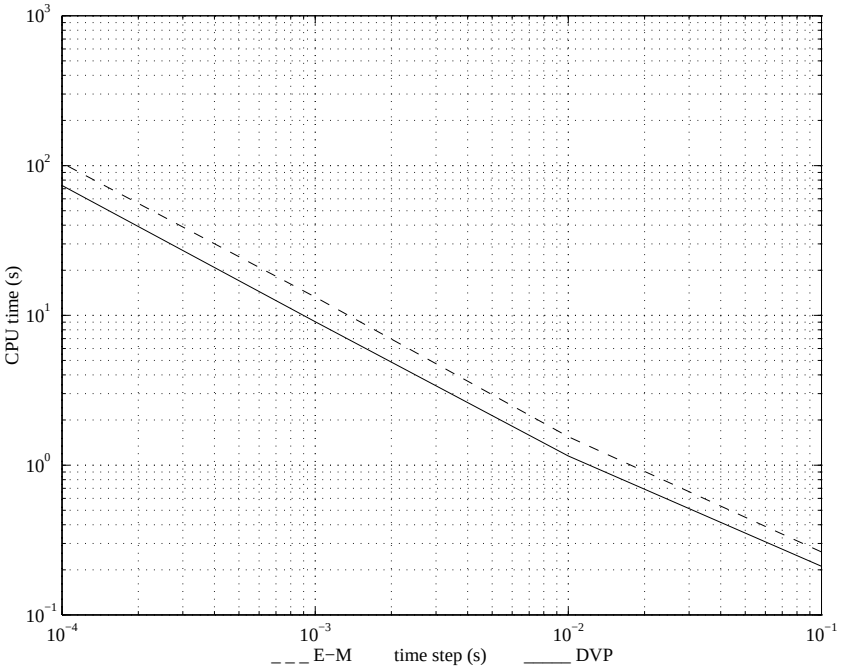

Fig. 7. CPU Time Versus Time Step for the DSP Simulation

formed by stacking p_1 and p_2, and

$$p_i^{n+\frac{1}{2}} = \frac{1}{2}\left(p_i^{n+1} + p_i^n\right).$$

The following parameters are used for the DSP: $m_1 = 2.0$Kg, $m_2 = 3.5$Kg, $l_1 = 4.0$m, $l_2 = 3.0$m, and g $= 9.81$m/s^2. The initial conditions are $x_1 = 2.820$m, $y_1 = 0.025$m, $x_2 = 5.085$m, $y_2 = 0.105$m, $\dot{x}_1 = 3.381$m/s, $\dot{y}_1 = 2.506$m/s, $\dot{x}_2 = 2.497$m/s, and $\dot{y}_2 = 10.495$m/s. The position and velocity of the z-coordinate is determined from the constraints, and the z-coordinate for both masses is taken to be negative. The output of the EM simulation at a time step of 0.0001s is used as the standard and initializes the second step in the DVP simulations. The results of the EM simulations and the DVP simulations are summarized in Table 5.2. The table contains the CPU time, position error, energy error and momentum error for the EM and the DVP simulations. The energy and momentum error for the EM simulations are zero. Equation (5.10) is used to calculate the errors for the DSP simulations.

Figure 7 is a plot of CPU time versus time step for the EM and DVP simulations. The DVP simulations are slightly faster for each time step and both CPU times drop off nearly linearly with increasing time step.

The position error for the EM and DVP simulations is shown in Figure 8. Both simulations show a second order relationship between position error and time step. The error for the EM simulation is slightly greater than the error

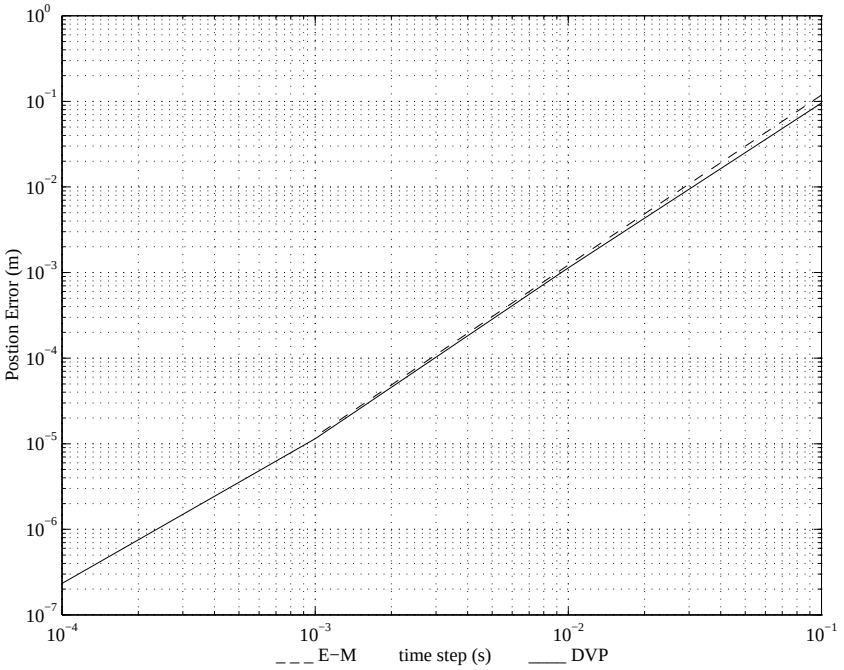

Fig. 8. Position Error Versus Time Step for the DSP Simulation

for the DVP simulation for $h \geq 10^{-3}$s.

Table 2
Simulation Results for the DSP Simulation

h (s)	Method	CPU time (s)	Pos. Error	Energy Error	Mom. Error
0.0001	DVP	73.648	2.329e-7	6.475e-6	2.547e-6
	EM	103.871	0.0	0.0	0.0
0.001	DVP	9.065	1.146e-5	3.269e-4	1.707e-4
	EM	13.250	1.214e-5	0.0	0.0
0.01	DVP	1.152	1.135e-3	3.224e-2	1.696e-2
	EM	1.549	1.225e-3	0.0	0.0
0.1	DVP	0.211	9.576e-2	2.665	1.560
	EM	0.263	1.184e-1	0.0	0.0

The y position of the second mass is shown in Figure 9 for the EM and DVP simulations for $h = 0.0001$s and $h = 0.1$s. Both the EM and DVP simulations at $h = 0.0001$s overlap and cannot be distinguished when plotted on the same graph. For both the EM and DVP simulations, reasonably accurate and fast trajectories are produced at large time steps, $h = 0.1$s. Both simulation methods may have uses in interactive simulation applications, such as design and animation, where real-time, reasonably accurate simulations are important.

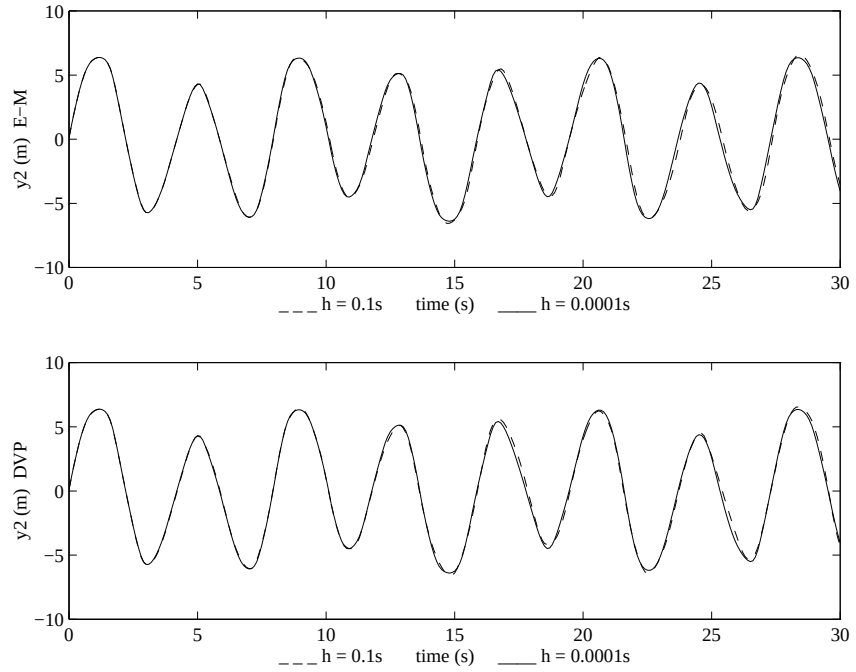

Fig. 9. Position Coordinate Versus Time for the DSP Simulation

The error in energy versus time step is shown in Figure 10. The DVP energy error appears to drop off as the square of the time step, at least for the large time steps. The energy error is zero for all time steps for the EM simulation. The energy for the DVP simulation at $h = 0.0001$s deviates between 24.944495109J and 24.944499828J and deviates between 20.910805793J and 25.583335766J for $h = 0.1$s.

The error in the momentum about the z-axis is shown in Figure 11. The momentum error for the EM simulation is zero for all time steps. The DVP algorithm should preserve momentum but for the smallest time step, $h = 0.0001$s, the momentum varies between 199.8254671770m^2/s to 199.8254671784m^2/s. The variation may be due to numerical errors. The momentum is constant for the other time steps. Again, the constant discrete momentum value approaches the value of the continuous momentum as the step size decreases.

Figure 12 shows the energy for the DVP simulations versus time for $h = 0.1$s and 0.01s in the lower graph. The upper graph shows energy versus time for $h = 0.001$s and 0.0001s. The energy oscillates about a constant value, and the constant value approaches the true energy. The amplitude of the oscillations decrease as the step size decreases. The fluctuations in energy appear to be related to the constraint forces. The middle graph is a plot of the multipliers versus time, and the fluctuations in the multipliers are correlated to the fluctuations in energy. This relationship has also been noticed in [4], and they use variable step size to decrease the energy oscillation.

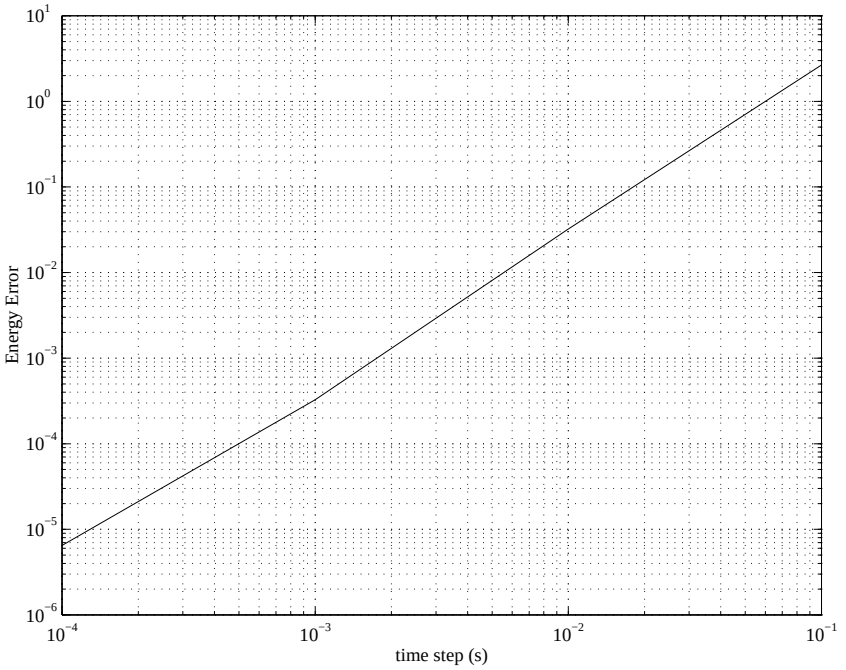

Fig. 10. Energy Error Versus Time Step for the DSP Simulation

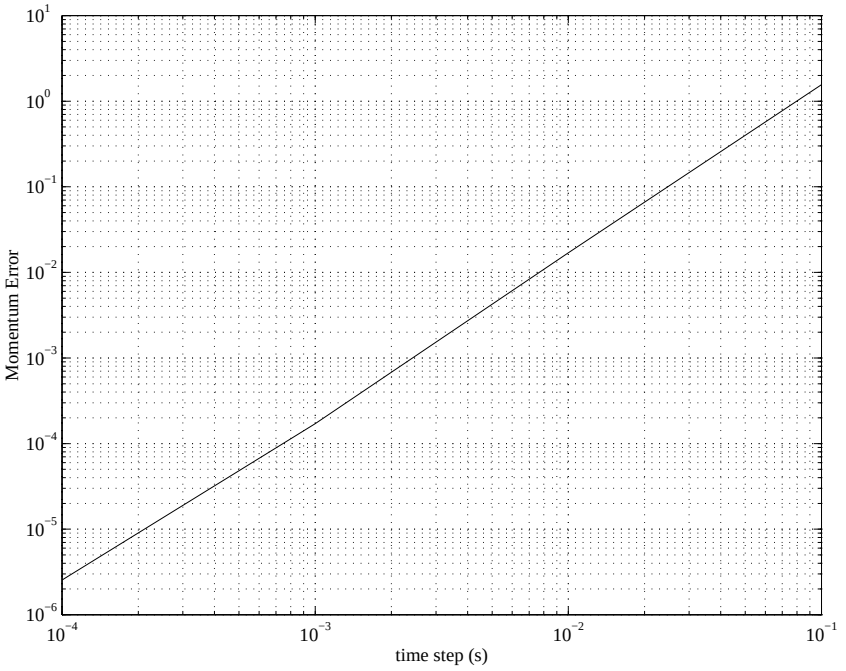

Fig. 11. Momentum Error Versus Time Step for the DSP Simulation

6 Conclusion

This paper first presented results on discrete mechanics and then presented a general method to construct symplectic-momentum mechanical integrators

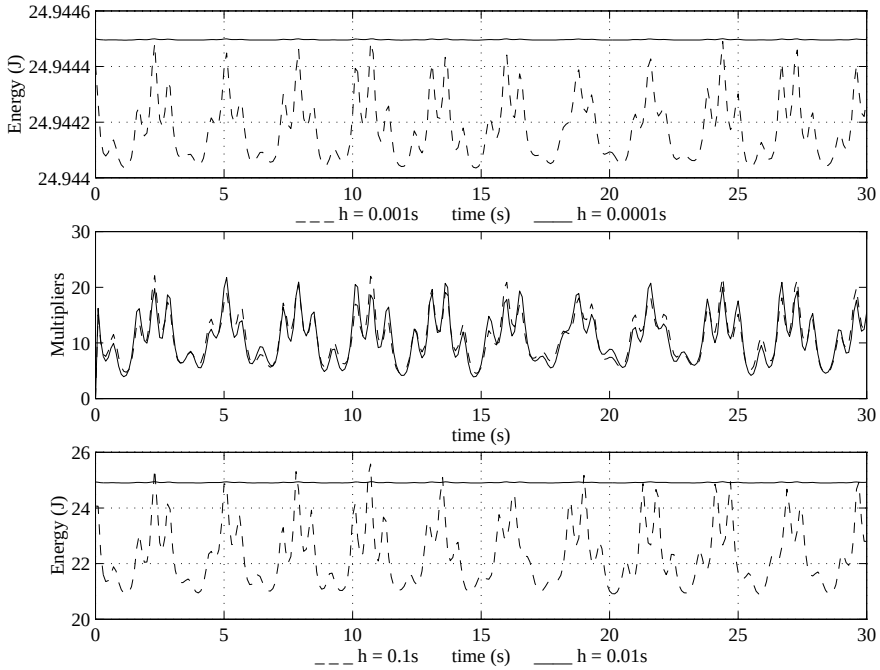

Fig. 12. Energy and Multipliers Versus Time for the DSP Simulation

for Lagrangian systems with holonomic constraints. The method was then applied to the rigid body and the double spherical pendulum. The discrete Euler-Lagrange (DEL) equations share similarities to the continuous equations of motion and preserve a symplectic form and invariants resulting from group invariance of the Lagrangian.

There are many areas of future work and development. We list a few of these here.

Energy-Momentum Integrators. One may proceed analogously to the derivation in this paper to create energy-momentum integrators possibly based on discretizing the principle of least action.

Nonholonomic Systems. The method presented in this paper treats holonomic constraints and one would like to generalize the method to treat nonholonomic constraints, as in [7]. For nonholonomic systems, the standard symplectic form is not preserved, and there are momentum equations and not conservation laws. Also, energy can be conserved in these systems. One has to develop algorithms taking into account these effects.

Multistep Methods and Time Step Control. It seems possible to modify the method to construct multistep mechanical integrators to increase the

accuracy of the method. One would also like to modify the method to allow variable time steps to improve efficiency.

External Forces. It would also be desirable to generalize the method to include external forces. This should be straightforward since they can be included in Hamilton's principle in standard fashion. One would also like to add control forces and dissipative forces to simulate controlled mechanical systems. The first author is currently using the techniques presented in this paper to develop a multibody simulator to simulate control systems for human models (see [51]).

Spacetime Integrators Since the method here is variational by nature and focuses on the temporal behavior, it should be helpful in the development of spacetime integrators by synthesis with existing finite element methods.

Acknowledgement

We first would like to thank Andrew Lewis for pointing out [3]. We would also like to thank Richard Murray and Abhi Jain for help with an initial investigation into mechanical integrators. We appreciate the useful comments and discussions provided by Francisco Armero and Oscar Gonzalez. We also thank Robert MacKay and Shmuel Weissman for useful discussions.

References

[1] H.C. Anderson. Rattle: A velocity version of the shake algorithm for molecular dynamics calculations. *Journal of Computational Physics*, 52:24–34, 1983.

[2] F. Armero and J.C. Simo. Long-term dissipativity of time-stepping algorithms for an abstract evolution equation with applications to the incompressible MHD and Navier-Stokes equations. *Computer Methods in Applied Mechanics and Engineering*, 131(1-2):41–90, 1996.

[3] J. C. Baez and J. W. Gilliam. An algebraic approach to discrete mechanics. Preprint, http://math.ucr.edu/home/baez/ca.tex, 1995.

[4] E. Barth and B. Leimkuhler. A semi-explicit, variable-stepsize integrator for constrained dynamics. Mathematics department preprint series, University of Kansas, 1996.

[5] E. Barth and B. Leimkuhler. Symplectic methods for conservative multibody systems. *Fields Institute Communications*, 10:25–43, 1996.

[6] G. Benettin and A. Giorgilli. On the Hamiltonian interpolation of near-to-the-identity symplectic mappings with application to symplectic integration algorithms. *Journal of Statistical Physics*, 74(5-6):1117–43, 1994.

[7] A.M. Bloch, P.S. Krishnaprasad, J.E. Marsden, and R.M. Murray. Nonholonomic mechanical systems with symmetry. *Archive for Rational Mechanics and Analysis*, 1996. To appear.

[8] P. Channell and C. Scovel. Symplectic integration of Hamiltonian systems. *Nonlinearity*, 3:231–259, 1990.

[9] A.J. Chorin, T.J.R. Hughes, J.E. Marsden, and M. McCracken. Product formulas and numerical algorithms. *Comm. Pure Appl. Math.*, 31:205–256, 1978.

[10] Z. Ge and J.E. Marsden. Lie-Poisson integrators and Lie-Poisson Hamilton-Jacobi theory. *Phys. Lett. A*, 133:134–139, 1988.

[11] R.E. Gillilan and K.R. Wilson. Shadowing, rare events, and rubber bands. A variational Verlet algorithm for molecular dynamics. *J. Chem. Phys.*, 97(3):1757–1772, 1992.

[12] O. Gonzalez. *Design and Analysis of Conserving Integrators for Nonlinear Hamiltonian Systems with Symmetry.* Ph.D. thesis, Stanford University, 1996. Department of Mechanical Engineering.

[13] O. Gonzalez. Time integration and discrete Hamiltonian systems. *Journal of Nonlinear Science*, 1996. To appear.

[14] T. Itoh and K. Abe. Hamiltonian-conserving discrete canonical equations based on variational difference quotients. *Journal of Computational Physics*, 77:85–102, 1988.

[15] L. Jay. Symplectic partitioned Runge-Kutta methods for constrained Hamiltonian systems. *SIAM Journal on Numerical Analysis*, 33(1):368–87, 1996.

[16] R. A. Labudde and D. Greenspan. Discrete mechanics-a general treatment. *Journal of Computational Physics*, 15:134–167, 1974.

[17] R. A. Labudde and D. Greenspan. Energy and momentum conserving methods of arbitrary order for the numerical integration of equations of motion-i. motion of a single particle. *Numer. Math.*, 25:323–346, 1976.

[18] R. A. Labudde and D. Greenspan. Energy and momentum conserving methods of arbitrary order for the numerical integration of equations of motion-ii. motion of a system of particles. *Numer. Math.*, 26:1–16, 1976.

[19] J.D. Lambert. *Numerical Methods for Ordinary Differential Systems.* John Wiley and Sons, New York, 1991.

[20] B. Leimkuhler and G. Patrick. Symplectic integration on Riemannian manifolds. *Journal of Nonlinear Science*, 6:367–384, 1996.

[21] B.J. Leimkuhler and R.D. Skeel. Symplectic numerical integrators in constrained Hamiltonian systems. *Journal of Computational Physics*, 112:117–125, 1994.

[22] D. Lewis and J.C. Simo. Conserving algorithms for the dynamics of Hamiltonian systems on Lie groups. *Journal of Nonlinear Science*, 4:253–299, 1995.

[23] H.R. Lewis and P.J. Kostelec. The use of Hamilton's principle to derive time-advance algorithms for ordinary differential equations. *Computer Physics Communications*, 1996. To appear.

[24] R. MacKay. Some aspects of the dynamics of Hamiltonian systems. In D. S. Broomhead and A. Iserles, editors, *The Dynamics of numerics and the numerics of dynamics*, pages 137–193. Clarendon Press, Oxford, 1992.

[25] S. Maeda. Lagrangian formulation of discrete systems and concept of difference space. *Math. Japonica*, 27(3):345–356, 1981.

[26] J. Marsden. *London Mathematical Society Lecture Note Series 174: Lectures on Mechanics*. Cambridge University Press, Cambridge, England, 1992.

[27] J. Marsden and T. Ratiu. *Introduction to Mechanics and Symmetry*. Springer-Verlag, New York, 1994.

[28] J.E. Marsden, G.W. Patrick, and W.F. Shadwick. *Integration Algorithms and Classical Mechanics*. Fields Institute Communications. American Mathematical Society, 1996. Vol. 10.

[29] J.E. Marsden and J. Scheurle. Lagrangian reduction and the double spherical pendulum. *Z.A.M.P*, 44(1):17–43, 1993.

[30] R. I. McLachlan and C. Scovel. A survey of open problems in symplectic integration. *Fields Institute Communications*, 10:151–180, 1996.

[31] R.I. McLachlan and C. Scovel. Equivariant constrained symplectic integration. *Journal of Nonlinear Science*, 5:233–256, 1995.

[32] J. Moser and A. P. Veselov. Discrete versions of some classical integrable systems and factorization of matrix polynomials. *Comm. in Mathematical Physics*, 139(2):217–243, 1991.

[33] R. Murray, Z. Li, and S. Sastry. *A Mathematical Introduction to Robotic Manipulation*. CRC Press, Boca Raton, Fl, 1994.

[34] M. Ortiz. A note on energy conservation and stability of nonlinear time-stepping algorithms. *Computers and Structures*, 24(1):167–168, 1986.

[35] S. Reich. Symplectic integration of constrained Hamiltonian systems by Runge-Kutta methods. Technical Report 93-13, University of British Columbia, 1993.

[36] S. Reich. Momentum preserving symplectic integrators. *Physica D*, 76(4):375–383, 1994.

[37] S. Reich. Symplectic integration of constrained hamiltonian systems by composition methods. *SIAM J. Numer. Anal.*, 33:475–491, 1996.

[38] S. Reich. Symplectic integrators for systems of rigid bodies. *Fields Institute Communications*, 10:181–191, 1996.

[39] J. Ryckaert, G. Ciccotti, and H. Berendsen. Numerical integration of the cartesian equations of motion of a system with constraints: molecular dynamics of n-alkanes. *Journal of Computational Physics*, 23:327–341, 1977.

[40] J. M. Sanz-Serna. Symplectic integrators for Hamiltonian problems: an overview. *Acta Numerica*, 1:243–286, 1991.

[41] J. M. Sanz-Serna and M. P. Calvo. *Numerical Hamiltonian Problems.* Chapman and Hall, London, 1994.

[42] F.A. Scheck. *Mechanics: From Newton's Laws to Deterministic Chaos.* Springer-Verlag, Berlin, 1990.

[43] Y. Shibberu. Time-discretization of Hamiltonian systems. *Computers Math. Applic.*, 28(10-12):123–145, 1994.

[44] J. C. Simo and N. Tarnow. The discrete energy-momentum method. Conserving algorithms for nonlinear elastodynamics. *ZAMP*, 43:757–792, 1992.

[45] J.C. Simo and O. Gonzalez. Assessment of energy-momentum and symplectic schemes for stiff dynamical systems. In *ASME Winter Annual Meeting*, New Orleans, 1993. Nov. 28 - Dec. 3, 1993.

[46] J.C. Simo and K.K. Wong. Unconditionally stable algorithms for rigid body dynamics that exactly preserve energy and momentum. *International Journal for Numerical Methods in Engineering*, 31:19–52, 1991. Also see addendum, 33:1321-1323, 1992.

[47] L. Verlet. Computer experiments on classical fluids. *Phys. Rev*, 159:98–103, 1967.

[48] A. P. Veselov. Integrable discrete-time systems and difference operators. *Funkts. Anal. Prilozhen.*, 22(2):1–13, 1988.

[49] A. P. Veselov. Integrable Lagrangian correspondences and the factorization of matrix polynomials. *Funkts. Anal. Prilozhen.*, 25(2):38–49, 1991.

[50] J. M. Wendlandt. Pattern evocation and energy-momentum integration of the double spherical pendulum. MA thesis, University of California at Berkeley, 1995. Department of Mathematics, CPAM-656.

[51] J.M. Wendlandt and S.S. Sastry. Recursive workspace control of multibody systems: A planar biped example. In *IEEE Control and Decision Conference*, Kobe, Japan, 1996. Dec. 11-13, 1996.

[52] J. Wisdom and M. Holman. Symplectic maps for the n body problem. *Astronomical Journal*, 102(4):1528–1538, 1991.

[53] S. Wolfram. *Mathematica: A System for Doing Mathematics by Computer.* Addison-Wesley, RedWood City, second edition, 1991.

[54] H. Yoshida. Construction of higher order symplectic integrators. *Phys. Lett. A*, 150:262–268, 1990.